Remote Speed Control Method of Brushless DC Motor for Wheeled Robot Based on Embedded Wireless Communication Technology

Shao-yong Cao and Wei-Jie Tang(✉)

School of Industrial Automation,
Zhuhai College of Bejing Institute of Technology, Zhuhai 519085, China

Abstract. According to the functional requirements of mobile robot, a remote speed control method of Brushless DC motor for wheeled robot based on embedded wireless communication technology is designed. Compared with the traditional microcontroller, using high-performance DSP2812 as the CPU of the robot simplifies the peripheral circuit and improves the high integration and stability of the method. At the same time, embedded wireless communication technology and fuzzy PID control algorithm are used to make up for the defect of single control algorithm and improve the dynamic performance of motor. The experimental results show that the remote speed control method of Brushless DC motor for wheeled robot based on embedded wireless communication technology improves the speed and control accuracy of motor, and improves the motion performance of robot.

Keywords: Embedded · Wireless communication · Wheeled robot · DC motor · Speed control

1 Introduction

The DC motor of wheeled robot has the characteristics of simple structure, strong stability, wide speed range and large output torque. It is widely used in drilling exploration, metallurgical processing, medical equipment, intelligent robot and other fields, and has achieved good results. For DC motor, accurate speed regulation is particularly important. In the early days, the DC motor speed control method of wheeled robot was generally realized by the circuit built by the simulator, which had limited speed range and low precision. After the birth of single chip microcomputer, there are many DC motor speed control methods with single chip microcomputer as the control core [1]. These methods take the speed of the motor as the controlled object, take the speed and current of the motor as the feedback of the method, and use PID and other conventional control methods to realize the accurate speed regulation of the DC motor. However, with the increase of the complexity of industrial production process, the traditional control method has been unable to adapt, so more complex control algorithm must be adopted [2]. Because of the limitation of memory space of MCU, these advanced algorithms can't work. Therefore,

S. Liu and X. Ma (Eds.): ADHIP 2021, LNICST 417, pp. 87–99, 2022.
https://doi.org/10.1007/978-3-030-94554-1_8

the DC motor speed control method based on arm, DSP and embedded wireless communication emerges as the times require, which provides higher control precision and wider speed range. The emergence of embedded wireless communication technology solves this problem and provides a new idea for precise speed regulation of DC motor. The traditional PLL circuit is basically analog-to-digital hybrid circuit [3]. Although the steady-state performance is good, the dynamic performance and anti-interference ability are poor. Based on the above analysis, in order to ensure that the DC motor speed control method can provide better speed control performance, and ensure that the method can run more complex control algorithm, this paper designs a remote speed control method of Brushless DC motor for wheeled robot based on embedded wireless communication technology [4]. Firstly, the brushless DC motor of wheeled robot is debugged, and then the parameters of the brushless DC motor are optimized. By controlling two quantities of current, the speed regulation of the brushless DC motor for wheeled robot is realized.Embedded wireless communication is used to realize high precision all digital phase locked loop technology and PWM motor drive signal. DSP is used to generate high-precision high-speed reference signal to form a set of high-performance DC motor speed control method.

2 Long-Distance Speed Control Method of Brushless DC Motor for Wheeled Robot

2.1 Transfer Function of Long-Distance Speed Regulation of DC Motor

In the speed regulation method of DC motor of wheeled robot, most of the motors are separately excited DC motors, and their equivalent circuits are shown as follows (Fig. 1):

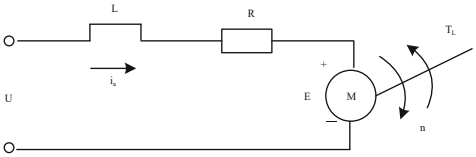

Fig. 1. Equivalent control circuit of DC motor

In most cases, the debugging method of Brushless DC motor for wheeled robot adopts variable voltage to realize the speed regulation of DC motor, so the input of the method is armature voltage m, and the output of the method is motor speed n. It can be seen from the figure that the armature voltage u is equal to the sum of the motor armature back electromotive force e, the resistance R voltage and the inductance l voltage, namely:

$$e + i_a R + L\frac{\mathrm{d}i_a}{\mathrm{d}t} = u \tag{1}$$

Among them, the motor armature back electromotive force e can be calculated by the following formula:

$$\mathrm{e} = \mathrm{C_e n/u} \tag{2}$$

Where g is the electromotive force constant of the motor. Based on this, the physical equation of motor can be obtained as follows:

$$C_e n + i_a R + L\mathrm{e}\frac{\mathrm{d}i_a}{\mathrm{d}t} = \Delta u \tag{3}$$

In addition, under the ideal no-load condition, the mechanical motion equation of the brushless DC motor for wheeled robot is known as:

$$T_e - T_L = \frac{GD^2}{375}\frac{\mathrm{d}n}{\mathrm{d}\Delta ut} \tag{4}$$

Where T = Cn is electromagnetic torque; TL is motor torque; GD2 is flywheel inertia, then.

$$T_i T_m \frac{\mathrm{d}^2 n}{\mathrm{d}t^2} + T_m \frac{\mathrm{d}n}{\mathrm{d}t} + n = \frac{u}{C_e} \tag{5}$$

In which:

$$T_i = \frac{L}{R} \tag{6}$$

$$T_m = \frac{GD^2}{375}\frac{R_d}{C_m C_e} \tag{7}$$

After further optimization, the transfer function of the motor mathematical model can be obtained:

$$W(s) = \frac{X_c}{X_r} = \frac{1/C_e}{T_d T_m s^2 + T_m s + 1} \tag{8}$$

Based on the above algorithm, the brushless DC motor for wheeled robot is calculated at a long distance to ensure the accuracy of control parameters.

2.2 Parameter Optimization of Brushless DC Motor for Wheeled Robot

Several optimization measures adopted in the structural design of the brushless DC motor for wheeled robots are further discussed, and some advantages of the brushless DC motor in operation are mentioned, and the performance of the motor with this structure in control is the focus of our further research [5]. In order to achieve good control of brushless DC motor for disc coreless wheeled robot, it is necessary to make a more in-depth theoretical discussion on its two main characteristics, coreless structure and array structure, which are different from ordinary disc motor, in order to provide a clear and reliable theoretical basis for the control application of this kind of motor, and standardize the basic design data of the motor based on this, as shown in the following Table 1:

Table 1. Basic parameters of brushless DC motor for wheeled robot

Design data	
Power (W)	200
Speed (R / min)	375
Phase number	3 (Y connection)
Input frequency (Hz)	50
Number of stator (module)	1
Polar logarithm	8
Number of coils (3 phases)	48
Turns per phase	640
Wire diameter (mm)	1 × 0.6
Inner diameter of permanent magnet (CM)	10.4
Outer diameter of permanent magnet (CM)	18
Air gap (CM)	0.8
Winding thickness (CM)	0.6
Thickness of permanent magnet (CM)	1.2
Efficiency (%)	80
power factor	0.99
Cooling system	Self cooling
Insulation class	F

For the brushless DC motor for wheeled robot, its permanent magnet rotor generates a constant magnetic field. When three-phase symmetrical current is applied to its three-phase symmetrical winding, a rotating magnetic field will be generated in the air gap [6]. According to the unified theory of motor, the two magnetic fields must remain relatively static to produce stable electromagnetic torque and drive the motor to rotate at synchronous speed [7]. Since the speed (frequency) of the stator magnetomotive force of the self-control synchronous motor is controlled by the rotor speed, the quantity that can be controlled is the amplitude and phase of the stator current. By controlling the two quantities of the current, the purpose of speed regulation of the brushless DC motor for wheeled robot can be achieved [8]. Based on this, the vector of the synthetic magnetomotive force of the stator is calculated

$$\overline{F_j^s} = N_s \bar{i}_j^{\bar{s}} = N_s \frac{3}{2} I_m e^{j(\lambda_0+\theta)} = F^s e^{j(\lambda_0+\theta)} \tag{9}$$

Where N is the number of turns of stator coil and the amplitude of stator magnetomotive force, I is the maximum value of phase current. The purpose of vector control

is to improve the performance of torque control, and the final implementation is still to control the stator current (AC). Because the physical quantities (voltage, current, electromotive force and magnetomotive force) on the stator side are all alternating current, and their space vectors rotate at synchronous speed in space, it is not convenient to adjust, control and calculate them. Therefore, coordinate transformation is needed to transform the physical quantities from static coordinate system to synchronous rotating coordinate system [9]. Use the information of numbers to record the shape of English or Chinese characters. See the table for the pin description of system operation (Table 2).

Table 2. Description of DC motor operation pin

Pin number	Pin name	Level	Pin function description
1	VSS	0V	Power ground
2	VCC	−5V	Power supply positive
3	V0	H/L	Contrast (brightness) adjustment
4	RS(CS)	H/L	Rs = "H" indicates that db7-db0 are display data Rs = "L" indicates that db7-db0 is the display instruction data
5	DB 0	H/L	Tri state data line
6	DB 1	H/L	Tri state data line
7	DB 2	H/L	Tri state data line
8	DB 3	H/L	Tri state data line
9	/RESET	H/L	Reset terminal, low level valid
10	VOUT	–	LCD driving voltage output terminal

Using single-chip microcomputer to drive stepping motor by software, not only can we freely set the speed, rotation angle and rotation times of stepping motor within a certain range through programming method, but also can conveniently and flexibly control the running state of stepping motor to meet the requirements of different users. Standing in the synchronous rotating coordinate system, each space vector of the motor becomes a static vector, and each space vector in the synchronous coordinate system becomes a direct flow. According to several forms of torque formula, the relationship between the torque and each component of the controlled vector can be found, and the component values of the controlled vector required for torque control can be calculated in real time. According to these given quantitative real-time control, the control performance of DC motor can be achieved.

2.3 Realization of Remote Speed Control of DC Motor

In the speed control of Brushless DC motor for wheeled robot, how to achieve high performance control of motor instantaneous torque is a key problem. The basic requirements of motor torque control are: fast response, high precision, small torque ripple, high efficiency and high power factor. The output torque control of Brushless DC motor

for wheeled robot can be attributed to AC / DC axial flow control [10]. Different combinations of transverse axial flow will affect the efficiency, power factor and output torque of the control mode. Based on the given torque, how to determine the AC and DC current is actually the problem of stator current vector control. The stator structure of asynchronous motor is similar to it. In the air gap, when the coil draws symmetrical AC current, it will produce the same rotating magnetic field as the induction motor. When the rotor has synchronous speed, the direction of the air gap magnetic field produced by the stator is the same, so the air gap magnetic field produced by the two rotors does not have relative speed, but has spatial potential angle difference. Two relatively static magnetic fields in the air gap interact to produce electromagnetic moment, which drives the rotor to rotate synchronously. When the stator current changes, the stator air gap magnetic field also changes, resulting in electromagnetic torque, which makes the load and speed different. Based on this, we need to further optimize the distribution structure of motor vector speed regulation (Fig. 2).

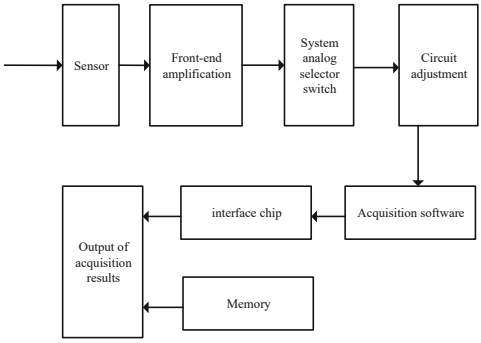

Fig. 2. Optimization of distribution structure of motor vector speed regulation

The adaptive compensation of microcontroller is a kind of multivariable and strongly nonlinear, so it is difficult to establish an accurate mathematical model [11]. This paper introduces the structure and classification of the self-adaptive compensation of single-chip microcomputer, gives the basic equations of the self-adaptive compensation under linear condition and ideal state, and establishes the mathematical model of the self-adaptive compensation after coordinate transformation. The controller module is mainly used to realize the motor speed control algorithm, but its output range does not match with the PWM module, so the designed controller module must be able to control the frequency of PWM signal output by the PWM module. The low frequency noise will be produced after the loop filter processing of the output of the frequency and phase detector. Therefore, the active p-type controller is used for further filtering processing, and its integral link can also effectively reduce the steady-state error. The active p-type controller also includes proportional link and integral link [12]. Using two adders and two multipliers, the pipeline computing process of embedded wireless communication can be easily realized.

The model equation of synchronous motor is not only complex, but also the degree of electric coupling is related to the rotor position, that is to say, the equation is indeterminate. The mathematical model of Brushless DC motor for wheeled robot in dq coordinate system can be obtained by coordinate transformation of stator equation of Brushless DC motor for wheeled robot in a, B and C coordinate system.

Voltage equation:

$$u_d = \frac{d\psi_d}{dt} - \omega\psi_q + R_1 i_d \tag{10}$$

$$u_q = \frac{d\psi_q}{dt} + \omega\psi_d + R_1 i_q \tag{11}$$

$$0 = \frac{d\psi_{2d}}{dt} + R_1 i_{2d} \tag{12}$$

$$0 = \frac{d\psi_{2q}}{dt} + R_1 i_{2q} \tag{13}$$

Flux linkage equation:

$$\psi_d = L_d i_d + L_{md} i_{2d} + L_{md} i_f \tag{14}$$

$$\psi_q = L_q i_q + L_{md} i_{2q} \tag{15}$$

$$\psi_{2d} = L_{2d} i_{2d} + L_{md} i_d + L_{md} i_f \tag{16}$$

$$\psi_{2q} = L_{2q} i_{2q} + L_{md} i_q \tag{17}$$

Electromagnetic torque:

$$T_{em} = p\left(\psi_d i_q - \psi_q i_d\right) \tag{18}$$

Mechanical motion equation:

$$J\frac{d\Omega}{dt} = T_{em} - T_L - R_\Omega \Omega \tag{19}$$

According to the vector control method of synchronous motor [13], the principle of vector control method is designed as shown in the Fig. 3.

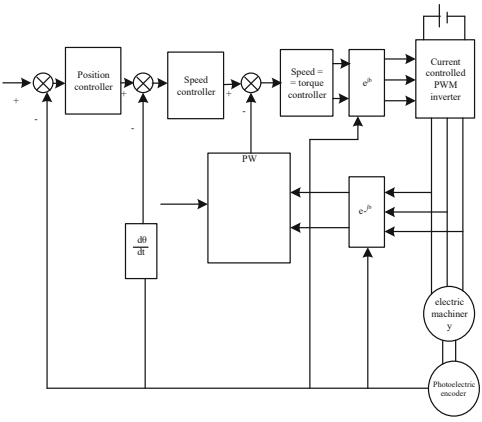

Fig. 3. Vector control principle of DC motor

In the figure, the rotor position sensor detects the position angle B of the brushless DC motor for the disc coreless wheeled robot, the torque controller controls the current, and the controllable PWM inverter supplies three-phase current to the brushless DC motor for the disc coreless wheeled robot. After the method initialization, the main program cyclically reads the control instruction (provided by SCI interrupt service program) and the motor speed data (provided by timer interrupt service program), and submits it to the Fuzzy-PID control algorithm module to calculate the new control quantity. The calculation result is sent to the comparison register, and PWM waveforms with different

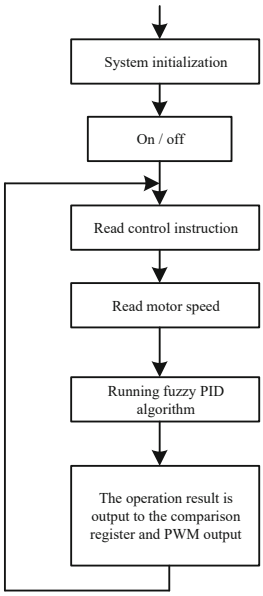

Fig. 4. Motor driver speed control step

duty ratios are output, and the motor speed is controlled by the motor driver. The specific steps are as follows (Fig. 4):

The single-step debugging method and full-speed debugging method are combined organically, so that it can find errors faster and more accurately than the single-step debugging method. Full-speed execution can be matched with set breakpoints to roughly determine the error range. Step-by-step can know the execution of each instruction in the program in detail, and you can easily know whether the instruction is correct by comparing the result of instruction running. On the basis of realizing the control of a single stepping motor, this method can also synchronously control multiple stepping motors. As shown in the following figure, further optimize the control of motor speed (Fig. 5):

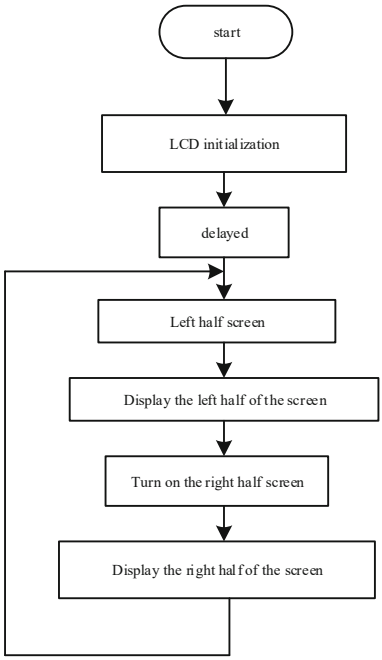

Fig. 5. Control steps of motor speed

Combining single-step debugging with full-speed debugging based on the above steps can make the whole debugging process find errors more quickly and accurately, thus improving the debugging efficiency. Full speed execution can be matched with set breakpoints to roughly judge the error range. By comparing the running results of instructions, we can know the running situation of instructions in the program, so it is easier to judge whether the instructions are correct or not. Taking a single stepping motor as the control object, the stepping motor of the multi-wheeled robot platform is synchronously controlled, so as to better improve the speed control effect of the DC motor of the wheeled robot and ensure the control accuracy.

3 Analysis of Experimental Results

Methods after the design is completed, in order to ensure the effect in energy saving, it needs to be applied to an example for simulation experiment. Only one diesel generator set is used in the experiment, and the parameters of main components are shown in the Table 3.

Table 3. Experimental parameters

Name	Parameter
Maximum engine power	80 KW
Generator efficiency	95%
Rated speed of generator	900 r·min^{-1}
Rated voltage of battery pack	350 V
Rated capacity of battery	100 Ah
Starting voltage of battery pack	50%

Generator set is composed of engine and generator. The fuel consumption of generator set is the fuel consumption of engine. The fuel consumption rate X of diesel engine can be regarded as a nonlinear function of speed s and torque Pi of diesel engine. The fuel consumption rate of the engine is:

$$X = f(P_i, s) \tag{20}$$

Assuming that the speed of the generator is fixed, the fuel consumption rate is a linear function of the engine power. The above speed identification algorithm is applied to the direct torque control method of Brushless DC motor for wheeled robot in the previous section, and the simulation is carried out. In the case of no-load and load, the waveforms of identification speed, actual speed and given speed are shown in the figure.

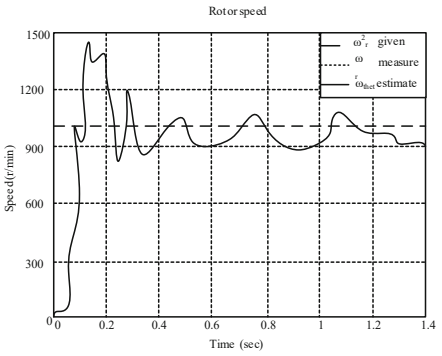

Fig. 6. Test results of traditional methods

The structure and principle of other parts of the simulation are the same as those in the previous section, which will not be repeated here (Figs. 6 and 7).

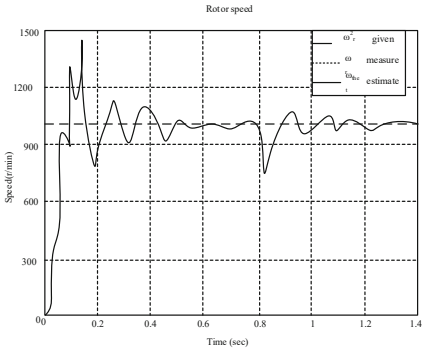

Fig. 7. The results of this method are as follows

It can be seen from the figure that during the speed rising period, the estimated speed is quite different from the actual speed value, especially when it rises to the maximum speed point. When the motor runs in steady state, the estimated speed is almost the same as the actual speed; When the load is running, especially when the speed fluctuates, the estimated speed can track the fluctuation of the actual speed in real time, which shows that the model reference adaptive speed estimation method has high dynamic performance. This is because DSP2812 is used as the CPU of the robot, which simplifies the peripheral circuit and improves the integration and stability of the method. Embedded wireless communication technology and fuzzy PID control algorithm are used to make up for the shortcomings of single control algorithm and improve the dynamic performance of the motor.

In order to further verify the effectiveness of this method, comparative experiments of motor control accuracy are carried out, and the control accuracy results of different methods are shown in Fig. 8.

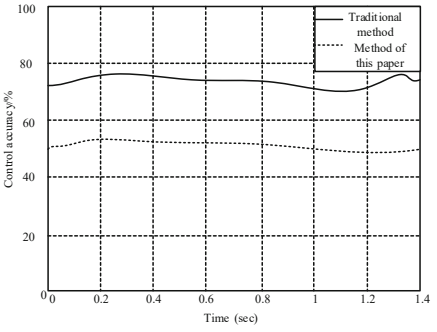

Fig. 8. Control accuracy results of different methods

As can be seen from Fig. 8, the motor control accuracy of the traditional method is about 50%, while the control accuracy of the method in this paper is about 75%, which indicates that the model reference adaptive speed estimation method has high control accuracy, and can ensure that the DC motor can effectively track the control target in the remote speed regulation.

4 Conclusion

Combined with embedded wireless communication technology, the remote speed control method of Brushless DC motor for wheeled robot is optimized. The method consists of two parts: control and drive. PLL and controller are implemented in FPGA. DSP is used to generate high accuracy reference signal. The design process of the method is introduced in detail. The high performance DSP2812 is used as the CPU of the robot, which simplifies the peripheral circuit and improves the integration and stability of the method. Embedded wireless communication technology and fuzzy PID control algorithm are used to make up for the shortcomings of single control algorithm and improve the dynamic performance of the motor.The simulation results show that the motor speed control method designed in this paper has good performance and can track the control target quickly.In the future development, this method will be applied to ensure the accuracy of the test, find out the details and further improve.

References

1. Chen, X., Liu, G., et al.: Sensorless optimal commutation steady speed control method for a nonideal Back-EMF BLDC motor drive system including buck converter. IEEE Trans. Industr. Electron. **67**(7), 6147–6157 (2019)
2. Song, W., Chen, H., Zhang, Q., et al.: On-chip embedded debugging system based on leach algorithm parameter on detection of wireless sensor networks. Math. Probl. Eng. **2020**(93), 1–7 (2020)
3. Zheng, S., Zheng, S.: Intelligent hospital and traditional Chinese medicine treatment of cerebrovascular dementia based on embedded system. Microprocess. Microsyst. **81**(1), 103661 (2021)
4. Qi, Z., Shi, Q., Zhang, H.: Tuning of digital PID controllers using particle swarm optimization algorithm for a CAN-based DC motor subject to stochastic delays. IEEE Trans. Industr. Electron. **67**(7), 5637–5646 (2020)
5. Chen, N., Jiao, X., Tan, R., et al.: A multi-parameter speed control model of traveling wave ultrasonic motor. Int. J. Appl. Electromagn. Mech. **64**(1–4), 457–464 (2020)
6. Das, S., Sarkar, P.P., Chowdhury, S.K.: Frequency tunable printed antenna with 90% size reduction for wireless communication applications. J. Instrum. **14**(11), 11010 (2019)
7. Bag, B., Biswas, P., Biswas, S., et al.: Wide-bandwidth multifrequency circularly polarized monopole antenna for wireless communication applications. Int. J. RF Microw. Comput.-Aided Eng. **29**(3), 21631.1–21631.11 (2019)
8. Alibakhshikenari, M., Khalily, M., Virdee, B.S., et al.: Double-port slotted-antenna with multiple miniaturized radiators for wideband wireless communication systems and portable devices. Prog. Electromagnet. Res. **90**(10), 1–13 (2019)
9. Shahjalal, M., Hasan, M.K., Chowdhury, M.Z., et al.: Smartphone camera-based optical wireless communication system: requirements and implementation challenges. Electronics **8**(8), 913–915 (2019)

10. Guerrero, E., Guzmán, E., et al.: FPGA-based active disturbance rejection velocity control for a parallel DC/DC buck converter-DC motor system. IET Power Electron. **13**(2), 356–367 (2020)
11. Liu, S., Liu, D., Srivastava, G., et al.: Overview and methods of correlation filter algorithms in object tracking. Complex Intell. Syst. **7**(3), 1895–1917 (2020)
12. Liu, S., Lu, M., Li, H., et al.: Prediction of gene expression patterns with generalized linear regression model. Front. Genet. **10**, 120 (2019)
13. Fu, W., Liu, S., Srivastava, G.: Optimization of big data scheduling in social networks. Entropy **21**(9), 902 (2019)